Desorption electrospray ionization mass spectrometry: Imaging drugs and metabolites in tissues

Justin M. Wiseman[a], Demian R. Ifa[b], Yongxin Zhu[c], Candice B. Kissinger[c,1], Nicholas E. Manicke[b], Peter T. Kissinger[a,c], and R. Graham Cooks[b,2]

[a]Prosolia, Inc., Indianapolis, IN 46202; [b]Department of Chemistry, Purdue University, West Lafayette, IN 47907; and [c]Bioanalytical Systems Inc., West Lafayette, IN 47906

Edited by Fred W. McLafferty, Cornell University, Ithaca, NY, and approved May 30, 2008 (received for review February 4, 2008)

Ambient ionization methods for MS enable direct, high-throughput measurements of samples in the open air. Here, we report on one such method, desorption electrospray ionization (DESI), which is coupled to a linear ion trap mass spectrometer and used to record the spatial intensity distribution of a drug directly from histological sections of brain, lung, kidney, and testis without prior chemical treatment. DESI imaging provided identification and distribution of clozapine after an oral dose of 50 mg/kg by: *i*) measuring the abundance of the intact ion at *m*/*z* 327.1, and *ii*) monitoring the dissociation of the protonated drug compound at *m*/*z* 327.1 to its dominant product ion at *m*/*z* 270.1. In lung tissues, DESI imaging was performed in the full-scan mode over an *m*/*z* range of 200-1100, providing an opportunity for relative quantitation by using an endogenous lipid to normalize the signal response of clozapine. The presence of clozapine was detected in all tissue types, whereas the presence of the *N*-desmethyl metabolite was detected only in the lung sections. Quantitation of clozapine from the brain, lung, kidney, and testis, by using LC-MS/MS, revealed concentrations ranging from 0.05 μg/g (brain) to a high of 10.6 μg/g (lung). Comparisons of the results recorded by DESI with those by LC-MS/MS show good agreement and are favorable for the use of DESI imaging in drug and metabolite detection directly from biological tissues.

pharmaceutical drugs | molecular imaging | tandem mass spectrometry | Clozapine

Mass spectrometry-based analytical methods have become standard in pharmaceutical research and product development laboratories. Specifically, liquid chromatography (LC) combined with tandem mass spectrometry (MS/MS) is commonly used for the analysis of lead compounds in drug discovery and development for metabolite identification, toxicology, and pharmacokinetic studies (1). The widespread use of MS in the drug discovery and development environment is a result of its high sensitivity, rapid analysis time, and the high specificity gained through employing MS/MS by using triple quadrupoles, Paul and Penning ion traps, and quadrupole TOF mass spectrometers. A major feature of the LC-MS/MS methodology is the requirement for relatively involved, destructive, and laborious sample preparation. For the analysis of tissue samples, these steps include homogenization and extraction of the target analyte(s), thereby precluding the opportunity to collect detailed histological information on the distribution or localization of drugs and their metabolites.

The information gained from determining the distributions of drugs and their metabolites in tissues and cells is important for understanding and predicting a drug's action and toxicity. Current methods for acquiring drug distributions in tissues include PET (2), MRI (3), and, most notably, autoradiography and fluorescence microscopy. Although PET and MRI can be used to perform *in vivo* studies, their main limitations are the relatively poor spatial resolution (on the order of millimeters) and, most significantly, the requirement for a radioactive label or reporter molecule for detection of the drug compound. Whole-body autoradiography (WBA) (4) is commonly used in the pharmaceutical industry because it provides quantitative, spatial information (on the order of micrometers) on drug compounds in relation to dose and time. WBA, however, also has significant limitations. As in PET, the drug compound must be derivatized to include a radioactive isotope for detection, making the procedure time-consuming, labor-intensive, and costly. Most significantly for both WBA and PET, it is the radioactivity of the label that is measured and not the intact drug molecule itself, making it difficult to distinguish between the drug and its metabolites.

MS imaging (5) has recently gained momentum, mainly because of continued improvements in MALDI and its application to direct tissue proteomics (6), but also because of the less widely recognized advances in secondary ion mass spectrometry (SIMS) (7). Whereas MALDI has been primarily used for profiling and imaging of peptides and proteins from tissues and cells, there is growing interest in applying MALDI to the analysis of small molecules, such as drugs and their metabolites (8–15). The development of small-molecule imaging by using MALDI has been challenging, primarily because matrix ions and mixed analyte-matrix clusters crowd the low-mass range, limiting confident detection of analyte ions of $<$750 Da. MS/MS approaches employing quadrupole TOF systems (13) or quadrupole ion traps (9, 15) have been used to circumvent this problem of signal-to-noise in the low-mass range. An alternative method to MALDI for small-molecule detection is desorption electrospray ionization (DESI) (16, 17), which also allows for direct analysis (18) and imaging (19) of biological tissues and other surfaces (20). In studies of model pharmaceutical compounds, the DESI signal response was shown to be linear ($R^2 = 0.996$), accurate (relative error $\pm$7%), and precise (relative standard deviation 7%) when analyzing neat solutions deposited on hydrophobic surfaces (21). DESI-MS imaging provides information on the spatial distribution of molecules at or near the surface with a lateral resolution that is currently $\approx$250 μm (22). DESI introduces some advantages over MALDI and SIMS imaging methods in that sample preparation is minimized and "soft" ionization allows intact molecules to be detected. These advantages are such that both DESI and the even newer ambient ionization method, laser ablation electrospray

Author contributions: C.B.K. and P.T.K. designed research; J.M.W., D.R.I., Y.Z., C.B.K., and N.E.M. performed research; J.M.W. and D.R.I. analyzed data; and J.M.W. and R.G.C. wrote the paper.

Conflict of interest statement: J.M.W. and P.T.K. are employed by Prosolia Inc, a manufacturer of DESI ion sources.

This article is a PNAS Direct Submission.

[1]Present address: The Chao Center for Industrial Pharmacy, Purdue Research Foundation, Department of Industrial Pharmacy, Purdue University, West Lafayette, IN 47906.

[2]To whom correspondence should be addressed. E-mail: cooks@purdue.edu.

This article contains supporting information online at www.pnas.org/cgi/content/full/0801066105/DCSupplemental.

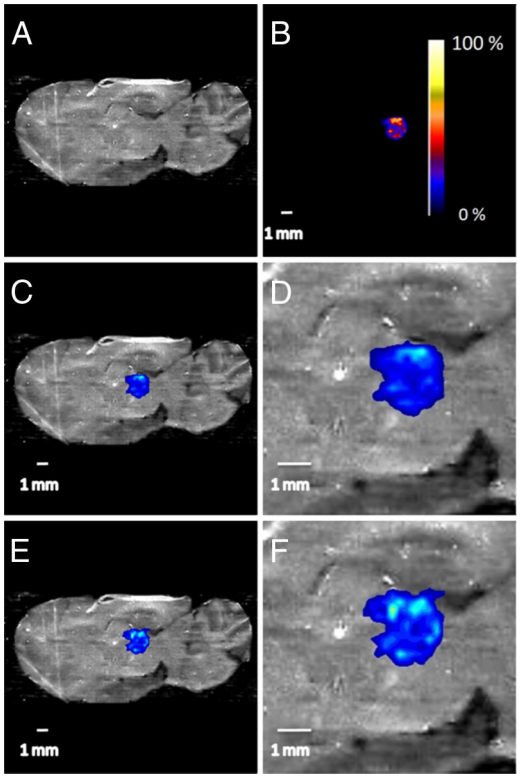

Fig. 1. Optical images of a sagittal rat brain section and overlayed images of clozapine deposited onto the tissue. (*A*) Optical image. (*B*) Interpolated image of an 1 μl deposit of 20 ng/μl solution of clozapine in acetonitrile; pixel size 245 μm $\times$ 245 μm; shown with intensity scale bar. (*C*) Overlay of the optical image in *A* and the clozapine image in *B*, shown on the same scale. (*D*) Zoom ($\times$3) of the overlayed images with 1-mm scale bar. (*E*) Overlay of the optical image in *A* and the clozapine image after a second scan. (*F*) Zoom ($\times$3) of the overlayed images with 1 mm scale bar.

ionization (LAESI), has been used for *in vivo* imaging experiments (23, 24). However, MALDI and, more particularly, SIMS offer much higher spatial resolution than DESI, which enables applications on the cellular (25) or subcellular levels (26). Nanostructure-initiator mass spectrometry (NIMS) has recently emerged as another new method for MS imaging, achieving a lateral spatial resolution of 150 nm (27). This new method allows for the analysis of samples with reduced fragmentation relative to SIMS and without a chemical matrix for ionization as used in MALDI, although unlike DESI, samples are examined in a vacuum.

Here, we report the application of DESI-MS for recording the spatial intensity distributions of the antipsychotic drug clozapine and its desmethyl metabolite directly from untreated, histological sections of brain, lung, kidney, and testis. The organs were divided into two equivalent sets with one-half being analyzed by DESI-MS imaging and the other by the standard method of LC-MS/MS. We show that the results obtained by using DESI-MS imaging of the intact tissue sections for clozapine correlate well with the results from LC-MS/MS, performed after homogenization and extraction of the other half of the same tissues from the same rat collected at the same time point. These results suggest the use of DESI-MS imaging in pharmacology, toxicology, and oncology as a means of seeking information about the tissue distribution of drugs and their metabolites or endogenous compounds without chemical treatment of any type.

Results and Discussion

Basic Concept and Strategy. DESI-MS is a new method of visualizing the tissue distributions of drugs and their metabolites, simultaneously and directly from an intact tissue section, without the need for chemical labeling or prior chemical treatment of the tissue. By scanning the charged-droplet beam across the tissue surface, molecular images are constructed by plotting the intensity of one or more of the ion signals derived from the surface, as a function of position. Because the DESI spray is a continuous flux of charged droplets, the surface is scanned unidirectionally at constant velocity (22, 28). In our experiment, the surface is moved from right to left, in the direction orthogonal to the inlet of the mass spectrometer, with the spray oriented toward the inlet, and the scanning pattern is such that it moves down the tissue sample from the spot, so as not to examine material that might have been contaminated when the previous row was examined. The experiment can be conducted in several operational modes: (*i*) full-scan MS, (*ii*) product scan MS/MS or MS^n, or (*iii*) multiple reaction monitoring (MRM) (29). Full-scan MS allows simultaneous mapping of multiple ions, whereas product scan MS/MS imaging isolates a particular ion or set of ions over a narrow *m/z* range and monitors characteristic fragment ions; both full-scan MS and MS/MS product ion scans are demonstrated here.

Table 1. Tissue and plasma concentrations of clozapine, determined by LC-MS/MS

Animal identification	Time, h	Brain, μg/g	Lung, μg/g	Kidney, μg/g	Testis, μg/g	Plasma, ng/mL
984	0	0	0	0	0	0
992	0.5	6.1	10.6	6.7	1.8	285.5
988	0.83	2.2	4	2.2	1.3	104.5
986	1.5	2.8	3.8	3	2.2	128.3
987	2	0.5	1.1	0.6	1.4	26.8
985	2.75	0.4	2	0.9	1.6	39.2
989	3	0.8	1.2	0.5	1.2	30.7
990	4	0.6	1.5	0.7	0.8	47.8
991	6	0.05	1.4	0.4	0.5	27.1
983	16	0.2	0.7	0.3	0.2	16.5

Method Development. In the DESI experiment, the charged droplets produced by the electrospray are pneumatically directed at high velocities (*ca.* 120 m/s) (30) toward the surface. In general terms, there are two possible outcomes that may result from droplets impinging onto a surface, deposition or splashing, with the latter resulting in secondary droplet formation (31). In both cases, prior droplet impact may have created a liquid film at the surface. The outcome of the impact is governed by the fluid properties (i.e., viscosity and surface tension) and kinematic parameters (i.e., droplet size and velocity), which are described by Reynolds and Weber numbers. Simulations of the DESI process indicate that the desorption event involves dissolution of the solid-phase analyte present at the surface into the deposited liquid film and its subsequent removal by splashing caused by impinging solvent droplets. Subsequently, ionization of analyte in the secondary droplets occurs by ordinary solvent evaporation and ion formation mechanisms that apply to conventional electrospray ionization (ESI), used to examine bulk solution-phase samples (32).

This mechanistic description of the DESI experiment and underlying processes is useful for method development purposes. In particular, in the imaging experiment, the spatial resolution may be degraded or the integrity of the sample may be compromised if significant redistribution of the analyte were to occur under particular experimental conditions (20, 33). To test this effect during tissue imaging, 1 μl of a clozapine solution (20 ng/μL) was deposited onto a rat brain section (Fig. 1*A*), allowed to dry, and analyzed in duplicate. The 1-μl droplet of clozapine produced a spot size $\approx$3.7 mm^2, resulting in a surface concentration of 5.4 ng/mm^2. Fig. 1*B* shows the DESI-MS/MS image of clozapine on the rat brain section that was recorded by using the conditions listed in Table S1. The

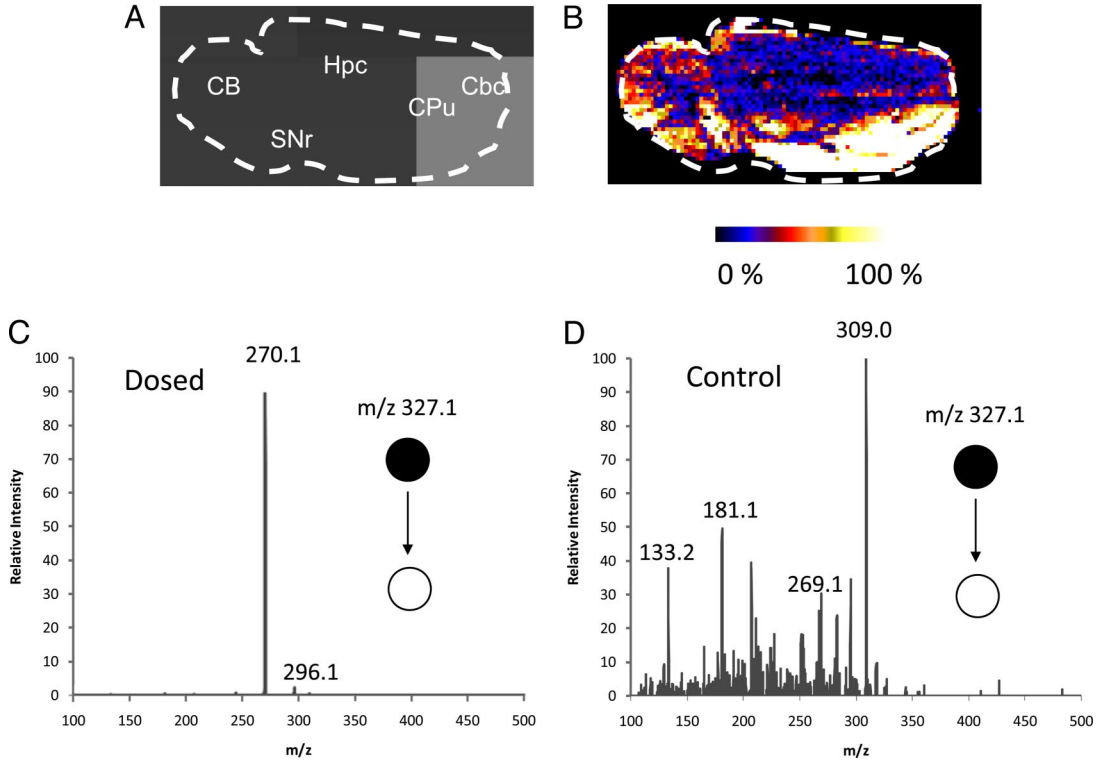

Fig. 2. Optical image of a 22 × 11 mm^2 sagittal rat brain section and the corresponding selected ion image. (*A*) Optical image of a sagittal rat brain section taken from animal 992 (0.5 h after dose). CB, cerebellum; Cbc, cerebral cortex; Cpu, caudate-putamen; Hpc, hippocampus; SNr, substantia nigra. (*B*) DESI mass spectral image of clozapine in the brain section recorded in MS/MS mode. The image of the fragment ion at *m/z* 270.1 is shown by using false colors in raw pixel format. (*C*) Average product ion mass spectrum of *m/z* 327.1 ± 2 in *B*. (*D*) Average product ion mass spectrum of *m/z* 327.1 ± 2 in control sample 984.

signal corresponding to clozapine is localized within the area in which it was originally deposited (Fig. 1 *C* and *D*). A second scan of the tissue section revealed that diffusion of clozapine, because of surface wetting or redistribution upon splashing, is insignificant (Fig. 1 *E* and *F*); that is, the spatial integrity of clozapine on the tissue section is retained under the chosen experimental conditions.

Imaging Clozapine in Rat Tissue. Clozapine [supporting information (SI) Fig. S1*A*], an atypical antipsychotic, binds preferentially to D_1-like dopamine receptors (including both D_1 and D_5 subtypes), which are found in relatively high density in the cerebral cortex, caudate putamen, accumbens nucleus, olfactory tubercle, and substantia nigra pars reticulate in both rat and monkey brains (34) but with less frequency in other areas of the brain, such as the cerebellum and striatum (*SI Text*). The major metabolic biotransformations of clozapine are to *N*-desmethylclozapine (NDC) (Fig. S1*B*) and clozapine-*N*-oxide (CLZ-NO) (Fig. S1*C*), reported to primarily be formed in the liver (35) and brain (36), respectively. Clozapine and its metabolites are strongly bound to plasma proteins, with the free fraction being <10% in the case of clozapine and NDC, and ≈25% for CLZ-NO (37). DESI-MS imaging was applied to visualize the distribution of clozapine in rat brain sections after the animals had been dosed and killed (Table 1). Fig. 2 shows the optical image (Fig. 2*A*) and the DESI image (Fig. 2*B*) from a rat brain section taken from an animal that had been dosed at 50 mg/kg via oral gavage and the brain removed 30 min after dose. The tissue was imaged in the MS/MS (29) mode, and the DESI product ion spectra resulting from fragmentation of clozapine at *m/z* 327.1 $(M+H)^+$ were recorded with a pixel size of 245 μm by 245 μm. The product ion mass spectrum shown in Fig. 2*C* is consistent with that of the authentic clozapine standard (Fig. S2*B*). The product ion mass spectrum recorded from control sample 984 (Table 1) is presented in Fig. 2*D* and does not show the presence of any characteristic product ions as displayed in Fig. 2*C*. The tissue was also imaged in the full-scan MS mode, but the signal-to-noise, in the absence of the chemical specificity of MS/MS, was not sufficient to reconstruct an image for the drug. Although reports indicate the presence of CLZ-NO in the brain (36), it was not detectable in the present study when either full-scan MS or MS/MS was performed. The distribution of clozapine in the tissue section showed relatively high levels in areas of the brain corresponding to cortical regions, which is in general agreement with studies in monkeys (38). Clozapine was detected in all brain samples in the MS/MS mode, with the exception of sample 991 that corresponded to a low clozapine concentration of 0.05 μg/g. Although one would not expect the distribution of clozapine to be the same across species because of differences in receptor density and localization, some studies using antibody staining have shown that the regional distribution of D1-like dopamine receptor subtypes is consistent between the monkey and rat (39).

Gardiner *et al.* (40) reported that significant accumulation of clozapine occurs in lung tissue versus brain, kidney, and liver. DESI-MS imaging was applied here to study the clozapine distribution and its metabolites in lung tissue. A 10-μm lung tissue section taken from an animal at 30 min after dose was imaged by using a pixel size of 230 μm by 230 μm. Images were acquired across a wide mass range, *m/z* 200 to 1100. The averaged full-scan mass spectrum recorded from the tissue section is shown in Fig. 3*A*. The mass spectrum from the lung tissue shows the presence of many endogenous species, including lipids in the mass range from *m/z* 700 to 1000. The majority of these peaks correspond to phosphatidylcholine (PC) species occurring in the form $M+H^+$, $M+Na^+$, and/or $M+K^+$. The most intense signal in the *m/z* range, 700 to 1000, is associated with the ion at *m/z* 756.4; MS/MS of this ion results in an abundant peak at *m/z* 697.3, that corresponds to a loss of a

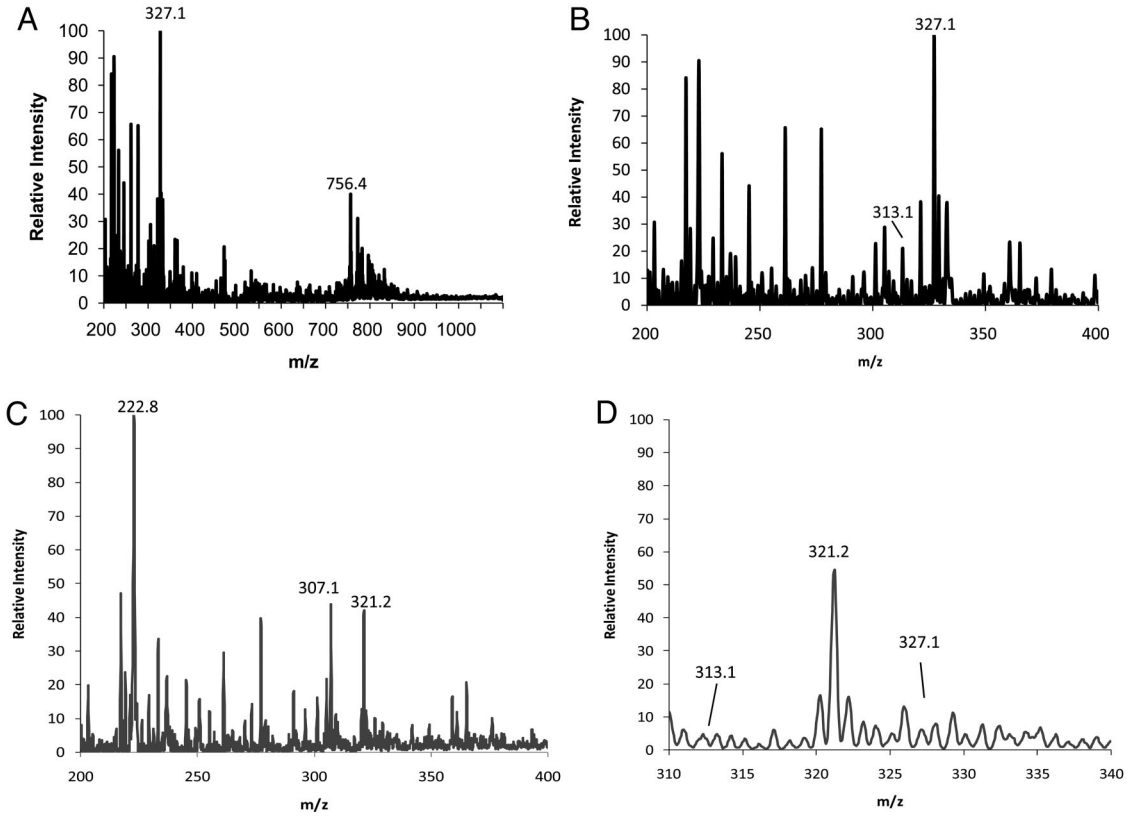

Fig. 3. Average mass spectra recorded in the positive ion mode of a lung tissue section. (*A*) Full mass spectrum covering the *m/z* range of 200-1100. (*B*) Full mass spectrum covering a *m/z* range of 200–400, showing the protonated clozapine ion $(M+H)^+$ at *m/z* 327.1 and the protonated desmethyclozapine (DMC) ion $(M+H)^+$ at *m/z* 313.1. (*C*) Full mass spectrum of control sample 984 covering the *m/z* range of 200–400. (*D*) Shown is the *m/z* range of 310–340, displaying the absence of clozapine and desmethylclozapine in the control.

neutral fragment of 59 Da (Fig. S3). Other major fragment ions of *m/z* 756.4 are *m/z* 573.4, *m/z* 551.4, and *m/z* 500.2, that correspond to losses of 183 Da, 205 Da, and 256 Da, respectively. The fragmentation pattern observed for *m/z* 756.4 is consistent with literature data on PCs, confirming that the observed ion is the sodiated form of a PC species (41–43), which we have assigned as PC (16:0/16:0). Clozapine ($[M+H^+] = 327.1$) and its *N*-desmethyl metabolite ($[M+H^+] = 313.1$) are clearly detectable in the lung tissue section as shown in the expanded mass spectrum in Fig. 3*B*. In contrast, neither the peak corresponding to clozapine nor that to desmethylclozapine is present in the control sample (Fig. 3 *C* and *D*). Additional mass spectral data for samples 988 and 986 of the rat lung is shown in Fig. S4 *A* and *B*. The corresponding images for clozapine, desmethylclozapine, and the PC (16:0/16:0) taken from full-scan MS spectra are shown in Fig. 4. Clozapine (Fig. 4*B*), desmethylclozapine (Fig. 4*C*), and the PC (16:0/16:0) (Fig. 4*D*) show relatively homogeneous distributions across the entire lung tissue section. The DESI-MS imaging and the corresponding LC-MS/MS results obtained in the complementary study confirm the presence of clozapine in the lung (Table 1). The LC-MS/MS also show that the concentration is much greater in the lung than in the brain, which is in agreement with Gardiner *et al.* (40).

To test whether the results obtained by DESI-MS imaging correlate with the concentrations determined by the more routine LC-MS/MS method, we recorded images for each lung tissue sample after the pharmacokinetic profile in the full-scan MS mode. In the full-scan DESI-MS mode, each pixel yields a full mass spectrum representing a wide range of *m/z* and intensity values. The DESI images were recorded on three serial sections and as the ratio of the peak intensity for *m/z* 327.1 to the peak intensity of *m/z* 756.4 (PC 16:0/16:0). The LC-MS/MS results reported here are expressed as micrograms of clozapine per gram of wet tissue (Table 1). The signal responses in each method were normalized to the maximum response in each experiment. The normalized signal responses were then plotted against the clozapine plasma concentrations as determined by LC-MS/MS (Table 1). Although not all time points could be tested by using the full-scan mode because of poor signal-to-noise for lower drug concentrations, the DESI results show a linear relationship to the plasma concentrations with $R^2 = 0.9669$ (Fig. 4*E*). The LC-MS/MS response versus the plasma concentrations was also linear with the plasma values having $R^2 = 0.9838$ (Fig. 4*E*). The significant, direct relationship between the tissue clozapine concentrations and the corresponding plasma levels is consistent with the available literature for olanzapine, a structural congener of clozapine (44). The relative concentration-time profile for clozapine in the lung, as recorded by using DESI in full-scan MS mode, indicates that the highest concentration found in the lung is 30 min after dose and that the terminal half-life ($t_{1/2}$) is between 0.75 and 1.5 h (Fig. S4*C*). This is also in general agreement with the LC-MS/MS results as shown in Table 1.

Additional studies were conducted on kidney and testis tissues. Investigations on the tissue distributions of clozapine had not shown the possibility of drug accumulation in the testis. The results from the DESI-MS/MS imaging of kidney and testis tissue sections 30 min after dose are shown in Fig. 5. Clozapine is clearly detectable in each tissue section with high specificity, because of the use of MS/MS mode imaging in these experiments. Its presence in both tissues is also confirmed by LC-MS/MS (Table 1). Each image was acquired in ≈30 min by using an image resolution of 44 × 29 pixels (pixel size: 345 μm × 345 μm) and 49 × 25 pixels (pixel size: 345 μm × 345 μm) for the kidney (Fig. 5*B*) and testis (Fig. 5*D*),

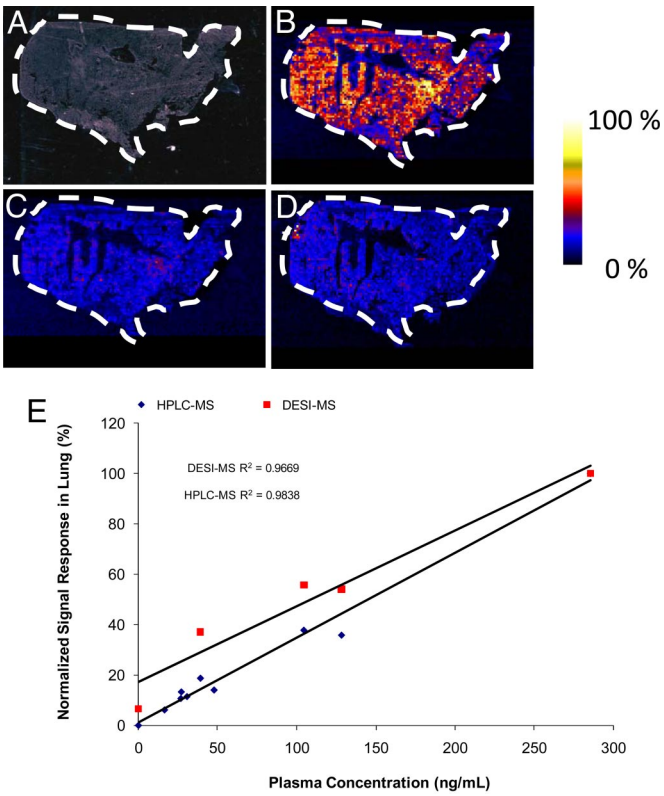

Fig. 4. Optical image of a 30.6 × 16.1 mm^2 lung tissue section and the corresponding selected ion images, each having 132 × 70 pixels and shown in false colors in raw pixel format. (*A*) Optical image. (*B*) Image of clozapine at *m/z* 327.1. (*C*) Image of desmethylclozapine at *m/z* 313.1. (*D*) Image of sodiated (M+ Na^+) PC 16:0/16:0 at *m/z* 756.4. (*E*) DESI-MS imaging and LC-MS/MS results of *D*. The signal responses in each method were normalized to the maximum response in each experiment. The normalized signal responses were then plotted against the clozapine plasma concentrations as determined by LC-MS/MS (Table 1).

respectively. In the kidney, clozapine was detectable in measurable amounts by using full-scan MS mode up to 2.75 h, excluding the 2.0 h time-point, and the relative concentration-time profile is consistent with the drug plasma levels (Fig. S5). Likewise, clozapine was detected in the testis in full-scan mode up to the 2.75 h time point.

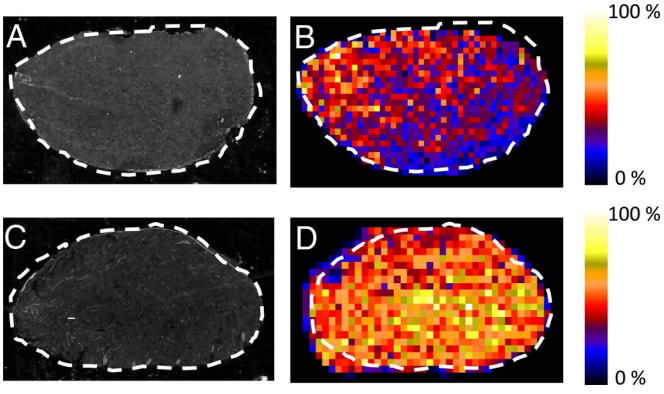

Fig. 5. Rat kidney and testis 0.5 h after dose. (*A*) Optical image of 10 μm rat testis section. (*B*) Corresponding DESI-MS/MS mass spectral image of clozapine for (*A*), represented by plotting the intensity of the characteristic fragment ion at *m/z* 270.1 arising from the mass-selected molecular ion at *m/z* 327.1 and shown in false colors in raw pixel format. (*C*) Optical image of 10-μm rat kidney section. (*D*) Corresponding DESI-MS/MS mass spectral image of clozapine for *C*, represented by plotting the characteristic fragment ion at *m/z* 270.1, arising from the mass-selected molecular ion at *m/z* 327.1 and shown in false colors in raw pixel format.

In conclusion, we demonstrated the capability for molecular imaging of small molecule pharmaceuticals and their metabolites directly from sections of biological tissue. By scanning the tissue sections with the DESI spray, we generated detailed spatial maps of many molecules simultaneously, obtaining molecular weight, intensity, and position information. This methodology has been confirmed by comparison with LC-MS/MS. The method presents some advantages over existing technologies used in bioanalysis; (*i*) it does not require the use of radioactive labels, (*ii*) it can be used to rapidly detect drug and metabolites simultaneously and display their spatial intensity distributions in two dimensions, directly from *untreated*, intact tissue sections, and (*iii*) it can reveal relative quantitative information on drugs and metabolites in tissues.

Although this method has these advantages, there are still potential limitations. Spectral overlap and ion suppression because of endogenous species of higher concentration and/or higher ionization efficiency increase the limit of detection in the full-scan MS mode. Limits of detection may be improved by using the MS/MS, MS^n, or MRM scan modes, but these approaches require *a priori* knowledge of the compounds of interest. In addition, the capability for determining the relative concentration of drugs and metabolites between organs is challenging because of tissue-specific ion suppression effects. However, methods to normalize signal responses recorded for different tissue types are already in use with MALDI, and they show results in good agreement with radiographic techniques (45).

Considering all these features, this method would appear to promise broad applicability in pharmacology, toxicology, and oncology. It has the advantage of limited sample preparation and, unlike traditional radiographic approaches, allows the simultaneous recording of molecular information for the drug molecule, its metabolites, and endogenous compounds.

Materials and Methods

Tissue Preparation. All experiments were performed in agreement with National Institutes of Health Guide for the Care and Use of Laboratory Animals and after approval from the local Institutional Animal Care and Use Committee. Ten male Sprague–Dawley rats (Harlan), ranging in weight from 261–286 g were used for the studies described. Nine animals were dosed orally at 50 mg/kg by using a 5-mg/ml solution of clozapine in acidified saline, pH 4.5, whereas one was not dosed and used as the control. At 0.5, 0.83, 1.5, 2.0, 2.75, 3.0, 4.0, 6.0, and 16.0 h after dose, the rats were euthanized by cardiac puncture under isofluorane anesthesia. The brain, lung, kidney, and testis were removed, immediately frozen over liquid nitrogen, and stored at −80°C. Half of each organ was allocated to LC-MS/MS and DESI-MS imaging, respectively. For DESI-MS imaging, the tissue samples were prepared by mounting the tissue on a small aliquot of optimal cutting medium and cutting each tissue to a thickness of 10 μm by using a cryomicrotome (Shandon, Thermo-Fisher Scientific). Each tissue section was thaw-mounted onto a plain microscope glass slide and analyzed without further processing.

DESI-MS Imaging. DESI-MS images were acquired by using a Thermo-Fisher Scientific LTQ linear ion trap mass spectrometer equipped with a prototype, automated DESI ion source. The studies described herein were conducted by using a spray solvent of 70:30 methanol:water in the positive ion mode; choices of other variables are displayed in Table S1. The DESI ion source used in these studies is similar to those reported for tissue studies (19). Images are acquired by continuously moving the surface beneath the spray at a constant velocity, over the whole tissue surface on a row-by-row basis. The pixel size is determined by the total scan time of the instrument and the surface velocity. Two operation modes were used for imaging. In full-scan MS mode, the surface scan rate in the x-dimension (orthogonal to the ion axis) was 200 μm/s and the step size in the y-dimension was 230 μm, resulting in a pixel size of 230 μm × 230 μm. Full-scan MS spectra were acquired over the *m/z* range of 200–1,100. In the product-scan MS/MS mode, the clozapine molecular ion at *m/z* 327.1 was selected by using a 2 mass unit window, and the fragment ion spectrum was recorded over a *m/z* range of 100–400. For the lung and brain samples, the surface scan rate was 200 μm/s, and the step size in the y-dimension was 245 μm, resulting in a pixel size of 245

μm $\times$ 245 μm. The time required for imaging the lung and brain samples was 180 and 80 min, respectively. For the kidney and testis samples, the surface scan rate in the x-dimension (orthogonal to the ion axis) was 300 μm/s, and the step size in the y-dimension was 345 μm, resulting in a pixel size of 345 μm $\times$ 345 μm. The time required for imaging the testis and kidney samples was 30 min for each sample. For the experiments on testis and kidney tissue sections, the pixel size was increased to reduce the time required for imaging because we did not expect to find the drug localized in the tissue substructure. In each imaging experiment, the data were acquired in profile mode, and automatic gain control (AGC) was turned off to ensure that the number of data points in each row of the image is consistent. An import filter for data conversion of Xcalibur™ raw data files from the Thermo-Fisher Scientific LTQ mass spectrometer into BioMAP 3.7.4.5 was written in-house.

LC-MS/MS. The other half of each tissue sample was weighed before homogenization and extraction (Table 1). To each tissue sample, 3.0 ml HPLC-grade methanol was added and homogenized with a Polytron aggregate equipped with a 7-mm blade (Polytron Inc.). Each solution was vortexed for 1 min, 0.7 ml of the homogenate was decanted into a nylon centrifuge filter (0.2 μm) and was centrifuged at 10,000 $\times$ *g* for 10 min at 4°C. Fifty microliters of the supernatant was mixed with 100 μl of mobile phase [methanol/0.1% formic acid (40:60 vol/vol)]. Quantitation was performed by using an external calibration at levels of 10, 100, and 1000 ng/ml clozapine with a Thermo-Fisher Scientific TSQ Quantum Ultra mass spectrometer by using selected reaction monitoring in the positive ion mode. Analytes were separated by using an Agilent Zorbax XDB-C18 (50 $\times$ 2.1 mm, 5 μm) column with a volumetric flow rate of 0.4 ml/min. The effluent from the HPLC was connected directly into the mass spectrometer by using an ESI source. The product ion transition monitored in the positive ion mode (+4.5 kV) was *m/z* 327.06→270.018 for clozapine by using a collision energy of 24 eV. For the plasma sample, an internal standard (loxapine, MW: 326.81, Sigma Aldrich) was used. A volume of 100 μl of plasma was mixed with a 50 μl loxapine solution (100 ng/ml in methanol) and 250 μl of methanol. Each solution was vortexed for 1 min and then centrifuged at 3200 rpm for 10 min at 4°C. Finally, 100 μl of the supernatant was mixed with 100 μl of HPLC-grade water. Quantitation was performed by using the same instrumentation and conditions as described. The product ion transition was monitored in positive ion mode (+4.5 kV) 327.90→192.99 for internal standard loxapine by using collision energy of 41 eV.

ACKNOWLEDGMENTS. We thank Dr. Amber Pond (Department of Basic Medical Sciences, Purdue University) for the use of her laboratory for tissue preparation and Jim Burleigh and Candace Rhode (Bioanalytical Systems Inc.) for contributions in animal dosing and procurement. This work was supported by the Office of Naval Research Research Tools Program Grant N000140510454 and the 21st Century Research and Technology Fund.

1. Korfmacher WA (2005) *Using Mass Spectrometry for Drug Metabolism Studies*, ed Korfmacher WA (CRC Press, Boca Raton, FL), pp 1–34.
2. Eckelman WC (2003) *Positron Emission Tomography* (Springer, Godalming, Germany), pp 815.
3. Beckmann N, Laurent D, Tigani B, Panizzutti R, Rudin M (2004) Magnetic resonance imaging in drug discovery: Lessons from disease areas. *Drug Discovery Today* 9:35.
4. Solon EG, Balani SK, Lee FW (2002) Whole-body autoradiography in drug discovery. *Curr Drug Metab* 3:451.
5. McDonnell LA, Heeren RMA (2007) Imaging mass spectrometry. *Mass Spectrom Rev* 26:606–643.
6. Stoeckli M, Chaurand P, Hallahan DE, Caprioli RM (2001) Imaging mass spectrometry: A new technology for the analysis of protein expression in mammalian tissues. *Nat Med* 7:493–496.
7. Pacholski ML, Winograd N (1999) Imaging with mass spectrometry. *Chem Rev* 99:2977.
8. Bunch J, Clench MR, Richards DS (2004) Determination of pharmaceutical compounds in skin by imaging matrix-assisted laser desorption/ionization mass spectrometry. *Rapid Commun Mass Spectrom* 18:3051–3060.
9. Drexler DM, *et al.* (2007) Utility of imaging mass spectrometry (IMS) by matrix-assisted laser desorption ionization (MALDI) on an ion trap mass spectrometer in the analysis of drugs and metabolites in biological tissues. *J Pharmacol Toxicol Methods* 55:279–288.
10. Hsieh Y, Chen J, Korfmacher WA (2007) Mapping pharmaceuticals in tissues using MALDI imaging mass spectrometry. *J Pharmacol Toxicol Methods* 55:193–200.
11. Hsieh Y, *et al.* (2006) Matrix-assisted laser desorption/ionization imaging mass spectrometry for direct measurement of clozapine in rat brain tissue. *Rapid Commun Mass Spectrom* 20:965–972.
12. Khatib-Shahidi S, Andersson M, Herman JL, Gillespie TA, Caprioli RM (2006) Direct molecular analysis of whole-body animal tissue sections by imaging MALDI mass spectrometry. *Anal Chem* 78:6448–6456.
13. Reyzer ML, Hsieh Y, Ng K, Korfmacher WA, Caprioli RM (2003) Direct analysis of drug candidates in tissue by matrix-assisted laser desorption/ionization mass spectrometry. *J Mass Spectrom* 38:1081–1092.
14. Wang HY, Jackson SN, McEuen J, Woods AS (2005) Localization and analysis of small drug molecules in rat brain tissue sections. *Anal Chem* 77:6682–6686.
15. Troendle FJ, Reddick CD, Yost RA (1999) Detection of pharmaceutical compounds in tissue by matrix-assisted laser desorption/ionization and laser desorption/chemical ionization tanndem mass spectrometry with a quadrupole ion trap. *J Am Soc Mass Spectrom* 10:1315.
16. Takats Z, Wiseman JM, Gologan B, Cooks RG (2004) Mass spectrometry sampling under ambient conditions with desorption electrospray ionization. *Science* 306:471–473.
17. Cooks RG, Ouyang Z, Takats Z, Wiseman JM (2006) Ambient mass spectrometry. *Science* 311:1566–1570.
18. Wiseman JM, Puolitaival SM, Takats Z, Cooks RG, Caprioli RM (2005) Mass spectrometric profiling of intact biological tissue by using desorption electrospray ionization. *Angew Chem Int Ed* 44:7094–7097.
19. Wiseman JM, Ifa DR, Song Q, Cooks RG (2006) Tissue imaging at atmospheric pressure using desorption electrospray ionization (DESI) mass spectrometry. *Angew Chem Int Ed* 45:7188–7192.
20. Ifa DR, Gumaelius LM, Eberlin LS, Manicke NE, Cooks RG (2007) Forensic analysis of inks by imaging desorption electrospray ionization (DESI) mass spectrometry. *Analyst* 132:461–467.
21. Ifa DR, Manicke NE, Rusine AL, Cooks RG (2008) Quantitative analysis of small molecules by desorption electrospray ionization (DESI) mass spectrometry from PTFE surfaces. *Rapid Commun Mass Spectrom* 22:503–510.
22. Ifa DR, Wiseman JM, Song Q, Cooks RG (2007) Development of capabilities for imaging mass spectrometry under ambient conditions with desorption electrospray ionization (DESI). *Int J Mass Spectrom* 259:8–15.
23. Justes DR, Talaty N, Cotte-Rodriguez I, Cooks RG (2007) Detection of explosives on skin using ambient ionization mass spectrometry. *Chem Commun* 2142–2144.
24. Nemes P, Vertes A (2007) Laser ablation electrospray ionization for atmospheric pressure, in vivo, and imaging mass spectrometry. *Anal Chem* 79:8098–8106.
25. Pacholski ML, Cannon DM, Ewing AG, Winograd N (1999) Imaging of exposed headgroups and tailgroups of phospholipid membranes by mass spectrometry. *J Am Chem Soc* 121:4716–4717.
26. McDonnell LA, *et al.* (2005) Subcellular imaging mass spectrometry of brain tissue. *J Mass Spectrom* 40:160–168.
27. Northen TR, *et al.* (2007) Clathrate nanostructures for mass spectrometry. *Nature* 449:1033–1037.
28. Kertesz V, Van Berkel GJ (2008) Scanning and surface alignment considerations in chemical imaging with desorption electrospray mass spectrometry. *Anal Chem* 80:1027–1032.
29. Busch KL, Glish GL, McLuckey SA (1988) *Mass Spectrometry/Mass Spectrometry: Techniques and Applications of Tandem Mass Spectrometry* (VCH, New York).
30. Venter A, Sojka PE, Cooks RG (2006) Droplet dynamics and ionization mechanisms in desorption electrospray ionization mass spectrometry. *Anal Chem* 78:8549–8555.
31. Roisman IV, Tropea C (2005) Fluctuating flow in a liquid layer and secondary spray created by an impacting spray. *Int J Multiphase Flow* 31:179–200.
32. Takats Z, Wiseman JM, Cooks RG (2005) Ambient mass spectrometry using desorption electrospray ionization (DESI): Instrumentation, mechanisms and applications in forensics, chemistry, and biology. *J Mass Spectrom* 40:1261–1275.
33. Pasilis SP, Kertesz V, Van Berkel GJ (2007) Surface scanning of planar arrays of analytes with desorption electrospray ionization-mass spectrometry. *Anal Chem* 79:5956–5962.
34. Dawson T, Gehlert D, McCabe R, Barnett A, Wamsley J (1986) D-1 dopamine receptors in the rat brain: A quantitative autoradiographic analysis. *J Neurosci* 6:2352–2365.
35. Olesen OV, Linnet KJ (2001) Contributions of five human cytochrome P450 isoforms to the N-demethylation of clozapine in vitro at low and high concentrations. *J Clin Pharmacol* 41:823.
36. Fang J (2000) Metabolism of clozapine by rat brain: The role of flavin-containing monooxygenase (FMO) and cytochrome P450 enzymes. *Eur J Drug Metab Pharmacokinet* 25:109.
37. Schaber G, Stevens I, Gaertner HJ, Dietz K, Breyer-Pfaff U (1998) Pharmacokinetics of clozapine and its metabolites in psychiatric patients: Plasma protein binding and renal clearance. *Br J Clin Pharmacol* 46:453.
38. Chou Y-H, Halldin C, Farde L (2006) Clozapine binds preferentially to cortical D1-like dopamine receptors in the primate brain: A PET study. *Psychopharmacology* 185:29–35.
39. Ciliax BJ, *et al.* (2000) Dopamine D5 receptor immunolocalization in rat and monkey brain. *Synapse* 37:125–145.
40. Gardiner T, Lewis J, Shore P (1978) Distribution of clozapine in the rat: Localization in lung. *J Pharmacol Exp Ther* 206:151–157.
41. Domingues P, Domingues MRM, Amado FML, Ferrer-Correia AJ (2001) Characterization of sodiated glycerol phosphatidylcholine phospholipids by mass spectrometry. *Rapid Commun Mass Spectrom* 15:799–804.
42. Ho Y-P, Huang P-C (2002) A novel structural analysis of glycerophosphocholines as TFA/K^+ adducts by electrospray ionization ion trap tandem mass spectrometry. *Rapid Commun Mass Spectrom* 16:1582–1589.
43. Han XL, Gross RW (1995) Structural determination of picomole amounts of phospholipids via electrospray ionization tandem mass spectrometry. *J Am Soc Mass Spectrom* 6:1202–1210.
44. Aravagiri M, Teper Y, Marder SR (1999) Pharmacokinetics and tissue distribution of olanzapine in rats. *Biopharm Drug Dispos* 20:369–377.
45. Stoeckli M, Staab D, Schweitzer A (2007) Compound and metabolite distribution measured by MALDI mass spectrometric imaging in whole-body tissue sections. *Int J Mass Spectrom* 260:195–202.